



ARL-TR-7382 • Aug 2015



Vehicle Exhaust Waste Heat Recovery Model with Integrated Thermal Load Leveling

by Christopher P Migliaccio and Nicholas R Jankowski

Approved for public release; distribution unlimited.

NOTICES

Disclaimers

The findings in this report are not to be construed as an official Department of the Army position unless so designated by other authorized documents.

Citation of manufacturer's or trade names does not constitute an official endorsement or approval of the use thereof.

Destroy this report when it is no longer needed. Do not return it to the originator.



Vehicle Exhaust Waste Heat Recovery Model with Integrated Thermal Load Leveling

by Christopher P Migliaccio and Nicholas R Jankowski
Sensors and Electron Devices Directorate, ARL

REPORT DOCUMENTATION PAGE

Form Approved
OMB No. 0704-0188

Public reporting burden for this collection of information is estimated to average 1 hour per response, including the time for reviewing instructions, searching existing data sources, gathering and maintaining the data needed, and completing and reviewing the collection information. Send comments regarding this burden estimate or any other aspect of this collection of information, including suggestions for reducing the burden, to Department of Defense, Washington Headquarters Services, Directorate for Information Operations and Reports (0704-0188), 1215 Jefferson Davis Highway, Suite 1204, Arlington, VA 22202-4302. Respondents should be aware that notwithstanding any other provision of law, no person shall be subject to any penalty for failing to comply with a collection of information if it does not display a currently valid OMB control number.

PLEASE DO NOT RETURN YOUR FORM TO THE ABOVE ADDRESS.

1. REPORT DATE (DD-MM-YYYY) Aug 2015		2. REPORT TYPE Final		3. DATES COVERED (From - To)	
4. TITLE AND SUBTITLE Vehicle Exhaust Waste Heat Recovery Model with Integrated Thermal Load Leveling				5a. CONTRACT NUMBER	
				5b. GRANT NUMBER	
				5c. PROGRAM ELEMENT NUMBER	
6. AUTHOR(S) Christopher P Migliaccio and Nicholas R Jankowski				5d. PROJECT NUMBER	
				5e. TASK NUMBER	
				5f. WORK UNIT NUMBER	
7. PERFORMING ORGANIZATION NAME(S) AND ADDRESS(ES) US Army Research Laboratory ATTN: RDRL-SED-E 2800 Powder Mill Road Adelphi, MD 20783-1138				8. PERFORMING ORGANIZATION REPORT NUMBER ARL-TR-7382	
9. SPONSORING/MONITORING AGENCY NAME(S) AND ADDRESS(ES)				10. SPONSOR/MONITOR'S ACRONYM(S)	
				11. SPONSOR/MONITOR'S REPORT NUMBER(S)	
12. DISTRIBUTION/AVAILABILITY STATEMENT Approved for public release; distribution unlimited.					
13. SUPPLEMENTARY NOTES					
14. ABSTRACT A system-level model describing thermoelectric generator (TEG)-based vehicle engine exhaust waste heat recovery (WHR) is formulated, and the impact of using high effective thermal conductivity devices to spatially load level the hot side of the TEG array is evaluated. Because TEG material properties are extremely sensitive to temperature, load levelled WHR systems generate more power at a higher efficiency than traditional WHR systems. The importance of proper assumptions and accurate boundary conditions is highlighted, and directions for future research are identified.					
15. SUBJECT TERMS waste heat recovery, thermoelectric generator, vehicle exhaust					
16. SECURITY CLASSIFICATION OF:			17. LIMITATION OF ABSTRACT UU	18. NUMBER OF PAGES 22	19a. NAME OF RESPONSIBLE PERSON Christopher P Migliaccio
a. REPORT Unclassified	b. ABSTRACT Unclassified	c. THIS PAGE Unclassified			19b. TELEPHONE NUMBER (Include area code) 301-394-1103

Contents

List of Figures	iv
List of Tables	iv
1. Introduction	1
2. Model Formulation	2
3. Results and Discussion	6
3.1 TEG Analysis	6
3.2 WHR System Analysis	9
3.3 WHR Model Comparison	11
4. Conclusion	11
5. References	13
Distribution List	16

List of Figures

Fig. 1	TE generator module (9505/127/150B, Ferrotec) properties as a function of temperature. The lines are a second-order polynomial fit to data (from Goncalves et al. ¹⁶).	3
Fig. 2	a) Traditional and b) heat pipe assisted cross-flow configurations. c) Control volumes (CVs) used in the analysis.....	4
Fig. 3	TE generator module hot and cold side temperatures along the array length with case 1 exhaust and cooling loop conditions. The dashed lines indicate the average hot and cold side temperatures in the cross-flow arrangement.	7
Fig. 4	TE generator module a) ZT, b) power generation, and c) conversion efficiency along the array length with case 1 exhaust and cooling loop conditions. For the cross-flow and heat pipe arrangements, $R_{hot} = 2, 5, 10, 50$ K/W and $R_{hot} = 0.01, 0.05, 0.1, 0.5$ K/W, respectively.....	9
Fig. 5	a) Overall efficiency and b) power generation of the TE generator array for exhaust and cooling loop conditions 1–4 as a function of R_{hot} . c) Total heat for rejection on the coolant side of the heat exchanger. .	10

List of Tables

Table 1	Exhaust and cooling loop conditions	4
---------	-------------------------------------------	---

1. Introduction

In conventional vehicles using internal combustion engines, approximately 40% of the fuel chemical energy available is lost to the exhaust stream. Much effort has been directed at recovering some of this waste heat for conversion to useful energy.¹ One of the most commonly proposed methods for vehicle waste heat recovery (WHR) is the use of a thermoelectric generator (TEG),^{2,3} although other techniques have been suggested including thermodynamic power cycles⁴ and direct thermal coupling.⁵ Thermoelectric (TE) materials offer several advantages that make them particularly attractive for mobile applications including being lightweight, solid-state, and passive. This has the potential for producing a reliable, low complexity solution for the vehicle; however, current TEGs suffer from low conversion efficiencies, especially at elevated temperatures (exhaust gases can range from 800–1100 K).⁶ This creates a significant engineering challenge in integrating the TE to the exhaust system and identifying a useful configuration with respect to recovered power.⁷ While much effort is going into the improvement of TE material performance and several studies have shown the potential of TE materials with a dimensionless figure of merit $ZT > 1$, delivering these materials outside the laboratory environment has proven challenging.^{8,9} As such, implementing a TEG for vehicular exhaust energy recovery requires careful attention be paid to the thermal integration of the TEG so as to take maximum advantage of the conversion efficiency of available materials.

When designing a TE WHR system, care must be taken in making simplifying assumptions regarding both vehicle thermal and energy conditions and TEG operation. Because of the inherently low conversion efficiency of available TE materials, improper assumptions significantly alter the perceived benefit of a particular integration strategy. Many studies evaluating the viability of TEG WHR have made assumptions regarding the operating point of the TEGs, namely, fixed temperature conditions at the TEG hot and cold sides, constant TE properties, no consideration of heat rejection to the coolant loop or energy cost for rejecting that heat, no impact of exhaust heat exchange on engine performance, and no accounting for circuit losses in converting the electricity to usable form.^{10–16} In reality, vehicle exhaust conditions (temperature and enthalpy) vary widely with engine speed and load.¹⁷ As a result, recovery systems designed around the TEG best-case operating point achieve efficiency metrics on paper but fail to do so in practice, because real applications will spend little time at any particular operating point, much less the optimal one.

One possible method of addressing the first concern—spatial temperature non-uniformity along the exhaust stream—is to use a high thermal conductivity device

(e.g., heat pipes/vapor chambers or heat spreaders with integrated diamond layers or carbon nanotubes arrays) to load level the temperature of the TEG hot sides.^{18,19} The advantage of this would be more uniform power generation across the array of TEGs when compared to a configuration where TEGs along the length of the exhaust are exposed to progressively lower temperatures, which shifts the material properties and leads to non-uniform power generation. Additionally, it may prove to be a simpler and less expensive solution than trying to optimize the TEG material configuration to match the expected spatial temperature gradient down the length of the exhaust.

In this report, a heat transfer model of the TEG is constructed, and the impact of using high effective thermal conductivity devices to spatially load level the TE array is considered. We examine the effect of the exhaust stream to TEG hot side thermal resistance on temperature load leveling and demonstrate that TEG temperature profiles approach the commonly assumed constant temperature difference condition when heat spreading devices are used.

2. Model Formulation

One of the more complete system-level TEG WHR models in literature is that of Goncalves et al.^{Error! Bookmark not defined.} In order to facilitate comparison with their work, we use a similar TEG configuration. This study considers one 16 x 6 array of TEGs (9505/127/150B, Ferrotec, as shown in Fig. 1) integrated in cross-flow heat exchangers operating at steady-state and subject to various boundary conditions (Table 1). Traditional (Fig. 2a) and heat spreader assisted (Fig. 2b) arrangements are evaluated. In both cases, the heat flow path from the exhaust stream to the TEG hot sides is described by a thermal resistance R_{hot} , which is varied to capture the effect of a range of heat transfer techniques (e.g., surface enhancements, fins, interfacial thermal greases). For the traditional cross-flow case, the lowest R_{hot} evaluated for each set of boundary conditions yields $T_H \sim 500$ K, which is the upper limit for the TEG property data used. For the heat spreader assisted cases, the lowest R_{hot} evaluated (0.01 K/W) corresponds to an idealized “best case” scenario, as achieving it would require multiple densely finned heat pipes, a high forced convection coefficient (>250 W/m²K, the high end of the range suggested by Incropera and DeWitt²⁰), and no interfacial and spreading resistances. On the coolant side, a constant thermal resistance from the coolant stream to each module is taken as $R_{cool} = 0.625$ K/W, which corresponds to a convection coefficient $h = 1000$ W/m²K and a heat transfer area $A = 1.6 \times 10^{-3}$ m² equal to the footprint of a single module.

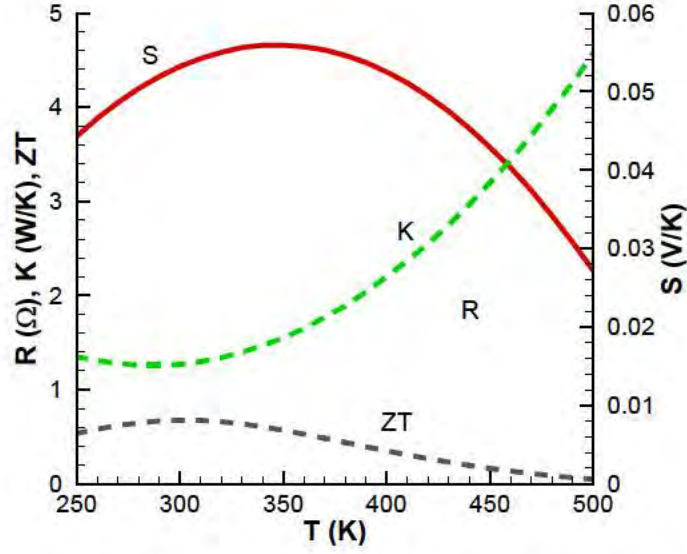


Fig. 1 TE generator module (9505/127/150B, Ferrotec) properties as a function of temperature. The lines are a second-order polynomial fit to data (from Goncalves et al.^{Error!} Bookmark not defined).

Table 1 Exhaust and cooling loop conditions

	\dot{m}_{exh} (kg/s)	$T_{exh, i}$ ($^{\circ}$ C)	\dot{m}_{cool} (kg/s)	$T_{cool, o}$ ($^{\circ}$ C)
case 1	0.02	650	0.15	65
case 2	0.01	580	0.15	65
case 3	0.01	580	0.15	50
case 4	0.02	650	0.15	50

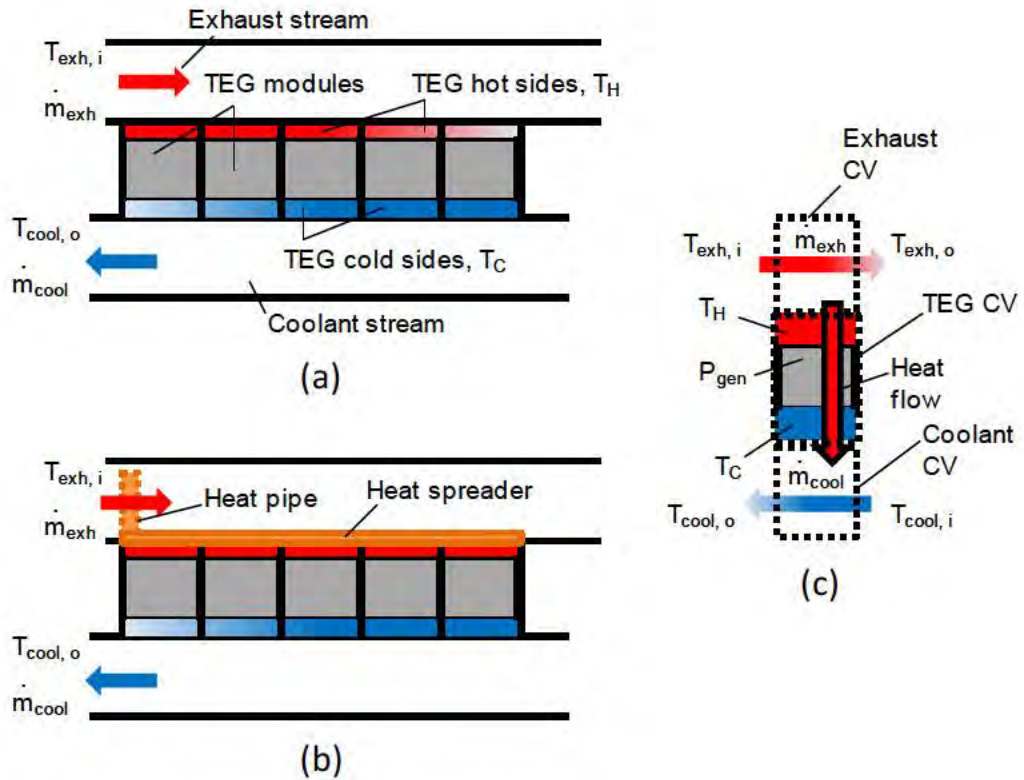


Fig. 2 a) Traditional and b) heat pipe assisted cross-flow configurations. c) Control volumes (CVs) used in the analysis.

$$\dot{m}_{exh} \quad \dot{m}_{cool}$$

The heat spreader assisted arrangement employs an integrated heat pipe and spreader assembly for temperature load leveling on the TEG hot sides. Due to the high effective thermal conductivity of the heat pipe,²¹ a lumped element approach is taken ($Bi < 0.1$ for heat pipe length < 2 m assuming an effective thermal conductivity of 5000 W/mK), and the heat pipe temperature is assumed to be a constant value determined by a separate iterative calculation that matches the exhaust heat extracted by the heat pipe to the total heat conducted through the TEG material in the module array. For simplicity, the thermal resistance R_{hot} accounts for all resistances between the exhaust stream and TE hot sides of the modules in the array. Heat spreaders can offer effective thermal conductivities of 10000 W/mK,²² thus, all TEG hot sides are assumed to be maintained at a constant temperature by a heat spreader.

Energy balances capturing the Seebeck effect and conduction through the TEG modules are performed on the control volumes illustrated in Fig. 2c. A system of equations is formulated (Eqs. 1–4) and solved using a Newton-Raphson iterative scheme.²³ TEG hot and cold side temperatures are assumed to be constant for each module, and all TEG module properties are evaluated using the average TEG temperature at the current iteration.

$$\frac{1}{R_{hot}} \left(\frac{T_{exh,i} + T_{exh,o}}{2} - T_H \right) = S I T_H + K(T_H - T_C) - I^2 R_{TE}/2 \quad (1)$$

$$\frac{1}{R_{cool}} \left(T_C - \frac{T_{cool,i} + T_{cool,o}}{2} \right) = S I T_C + K(T_H - T_C) + I^2 R_{TE}/2 \quad (2)$$

$$\frac{1}{R_{hot}} \left(\frac{T_{exh,i} + T_{exh,o}}{2} - T_H \right) = \frac{\dot{m}_{exh} c_{p,exh} (T_{exh,i} - T_{exh,o})}{r} \quad (3)$$

$$\frac{1}{R_{cool}} \left(T_C - \frac{T_{cool,i} + T_{cool,o}}{2} \right) = \frac{\dot{m}_{cool} c_{p,cool} (T_{cool,o} - T_{cool,i})}{r} \quad (4)$$

S and R_{TE} are the module Seebeck coefficient and electrical resistance, r is the number of rows in the TE array, and c_p is taken to be 1000 J/kg for the exhaust gas. The coolant c_p is evaluated at each iteration based on a 50:50 water:ethylene glycol mixture;²⁴ the coolant mass flow rate \dot{m}_{cool} is taken as 0.15 kg/s, equal to the midpoint of flow rates evaluated by Oliet et al.²⁵ The TEGs in the array are all connected in series; thus, the generated current I must be equal in all modules. This adds an additional constraint to the system of equations:

$$I = \frac{S(T_H - T_C)}{\frac{R_{load}}{n} + R_{TE}} \quad (5)$$

where n is the total number of TE modules and R_{load} is load resistance, assumed to be $R_{load} = \sum_1^n R_{TE}$.

The power generated by each TE module is¹¹

$$P_{gen} = S I (T_H - T_C) - I^2 / R_{TE} \quad (6)$$

The TE conversion efficiency η_{conv} of each TE module is evaluated by comparing the power generated to the input thermal power:²⁶

$$\eta_{conv} = \frac{P_{gen}}{K(T_H - T_C)} \quad (7)$$

The system conversion efficiency is calculated by comparing the total generated power $\sum_1^n P_{gen}$ to the exhaust enthalpy as

$$\eta = \frac{\sum_1^n P_{gen}}{\dot{m}_{exh} c_{p,exh} (T_{exh,i} - T_{amb})} \quad (8)$$

where T_{amb} is taken to be 300 K. Also of interest is the total heat for rejection on the TEG array coolant loop:

$$Q_C = \dot{m}_{cool} c_{p,cool} (T_{cool,o} - T_{cool,i}) \quad (9)$$

where $T_{cool,o}$ and $T_{cool,i}$ are evaluated at the array outlet and inlet, respectively.

3. Results and Discussion

3.1 TEG Analysis

Figure 3 presents the hot and cold side temperatures of TEG modules along the axial length of an exhaust for traditional and heat spreader assisted cross-flow configurations under case 1 boundary conditions. Without the integrated heat pipe and spreader assembly, the TEG module temperatures rapidly decline along the length of the exhaust pipe. The temperature non-uniformity is more pronounced at low R_{hot} because more heat is transferred from the exhaust stream, leading to higher module temperatures as the coolant outlet temperature remains constant. For both configurations, increases in R_{hot} diminish the TEG hot and cold side temperature difference, which adversely affects power generation (Eq. 6). Dashed lines in the figure are the average TEG hot and cold side temperatures, which are representative of the idealized case where a constant $\Delta T = T_H - T_C$ may be taken. It is seen that the heat pipe assisted configuration provides similar temperature profiles— T_H is constant due to the heat spreader and the rise in T_C along the TEG array is minimal due to the high coolant flow rate. This indicates that a heat pipe assisted cross-flow configuration can achieve results very close to the ideal constant ΔT case.

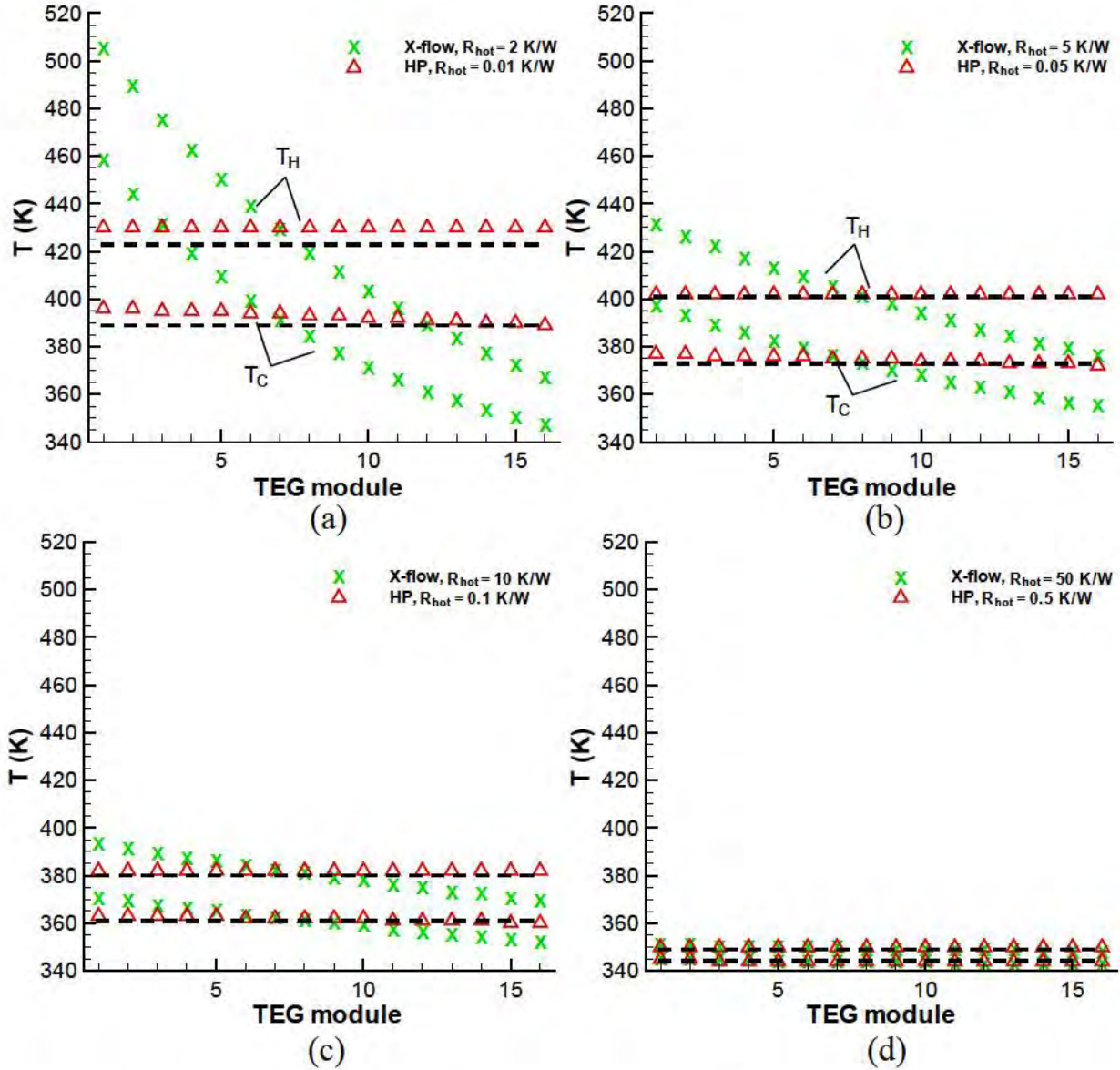


Fig. 3 TE generator module hot and cold side temperatures along the array length with case 1 exhaust and cooling loop conditions. The dashed lines indicate the average hot and cold side temperatures in the cross-flow arrangement.

The effect of non-uniform temperature on the TEG properties is captured by plotting ZT along the length of the exhaust pipe, as shown in Fig. 4a. Module ZT decreases sharply with increasing temperature (see Fig. 1); thus, cases with higher R_{hot} lead to higher ZT values. The generated power for each module is correlated to $S^2(T_H - T_C)^2$ (Eqs. 5 and 6). For traditional cross-flow configurations, the first modules in the array are subjected to the highest temperatures, and ΔT decreases along the length of the array. The first module at the lowest R_{hot} (2 K/W for case 1) yields low power generation and efficiency due to its very low value of S . As the

average module temperature decreases along the length of the TEG array, the power peaks and proceeds to decline toward the end of the array, yielding very non-uniform P_{gen} . Unlike the traditional cross-flow configuration, the heat pipe assisted system exhibits a ΔT that increases as the end of the TEG array is approached. This is due to the fact that T_H is leveled by the heat spreader, and the coolant flow enters the heat exchanger at the end of the array, thus yielding the largest ΔT in the system (Fig. 4b). TEG conversion efficiencies are below 1% for each module (Fig. 4c). Overall device efficiencies are even lower (Fig. 5a) indicating that the current system does a poor job of converting available exhaust enthalpy to usable power. Overall efficiency could be improved by adding more TEG arrays; however, extracting more heat from the exhaust stream would drop the TEG hot side temperatures (and thus shift the operating point of the TEG modules), meaning that the results of the present investigation cannot be directly extended to a multi-array system.

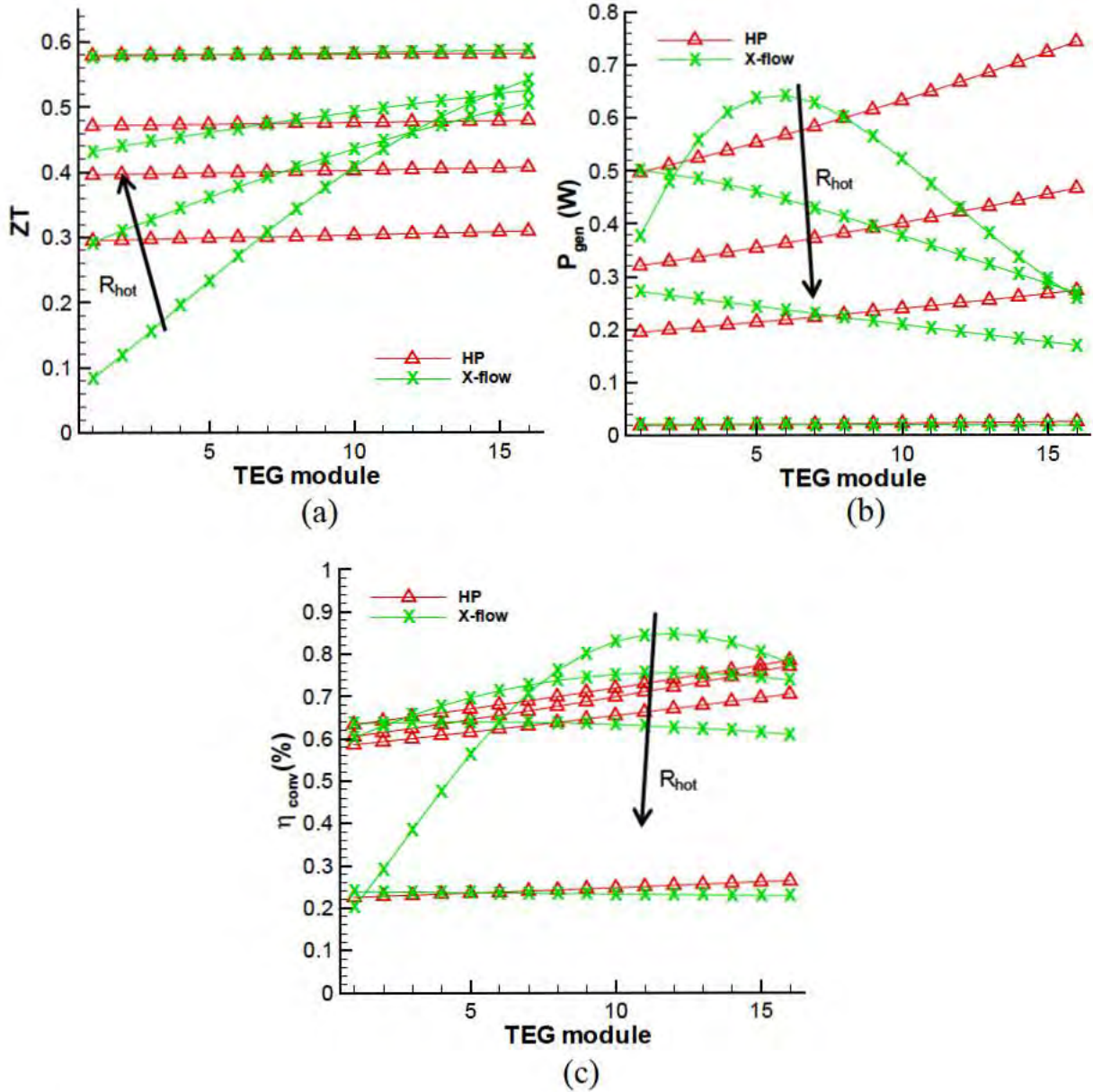


Fig. 4 TE generator module a) ZT, b) power generation, and c) conversion efficiency along the array length with case 1 exhaust and cooling loop conditions. For the cross-flow and heat pipe arrangements, $R_{hot} = 2, 5, 10, 50$ K/W and $R_{hot} = 0.01, 0.05, 0.1, 0.5$ K/W, respectively.

3.2 WHR System Analysis

It is worth examining the impact of the TEG WHR system on the rest of the system to better understand the net power generation provided. First, heat through the TEG not converted to useful power must be rejected by the coolant loop. Figure 5b–c presents the total system power generation and coolant loop heat rejection. Due to the low TEG conversion efficiencies, the maximum ratio of P_{gen} to Q_c achieved for

both cross-flow and heat pipe assisted configurations is 0.007, indicating that under the conditions of case 1 (the most optimistic scenario considered), 1000 W must be dissipated for every 7 W generated. Taking the generic radiator studied parametrically by Oliet et al.²⁵ and assuming adequate air flow over the radiator fins, the dissipation of 10 kW requires about 3 W of coolant pumping power, equal to $\sim 5\%$ of P_{gen} for the best-performing cases. This does not account for any additional fan power that may be required to generate the needed airflow, which may be significant.

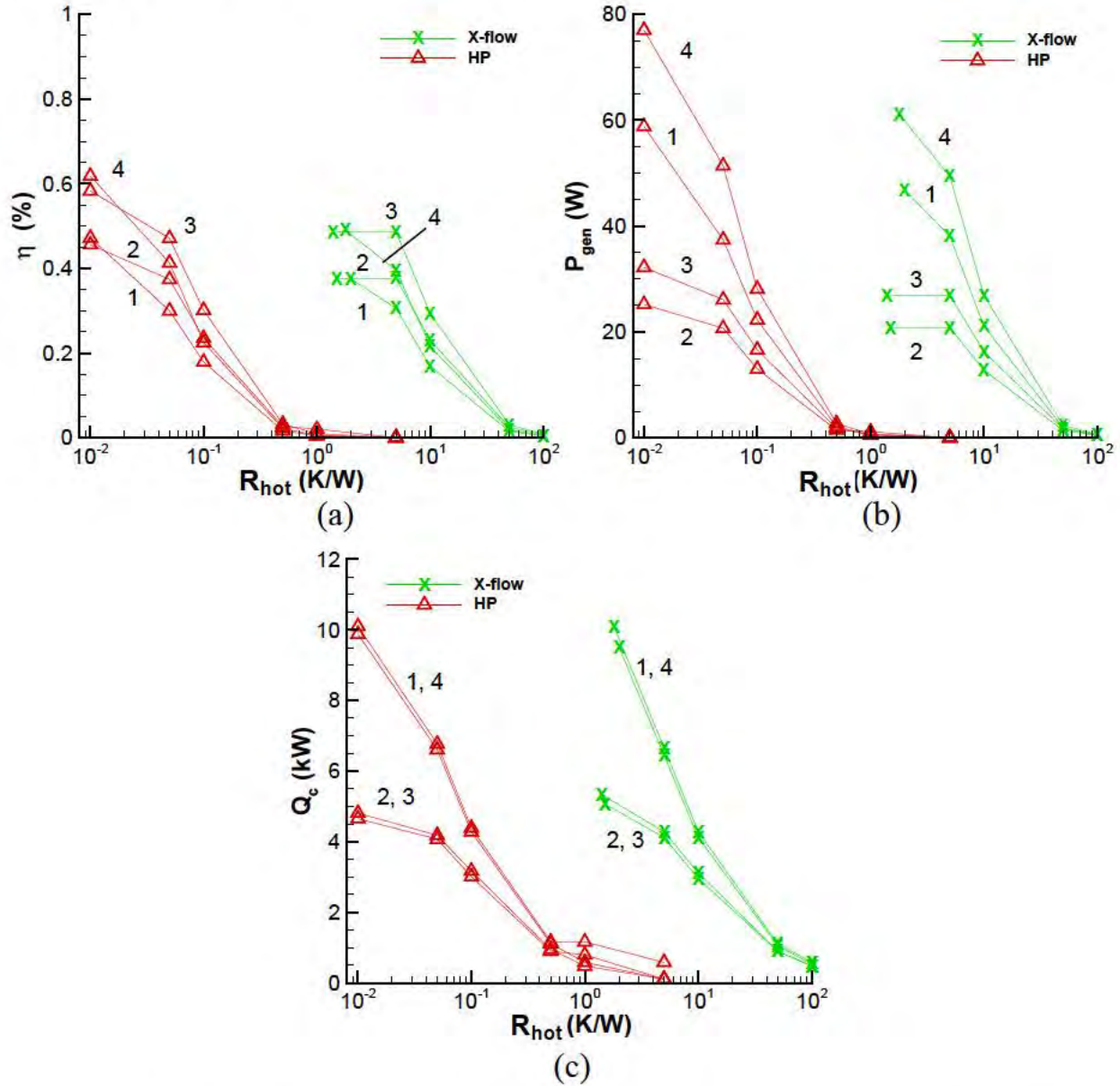


Fig. 5 a) Overall efficiency and b) power generation of the TE generator array for exhaust and cooling loop conditions 1–4 as a function of R_{hot} . c) Total heat for rejection on the coolant side of the heat exchanger.

A secondary system concern is the effect of the hot side heat exchanger on engine performance. Previous studies have shown that for a wide range of engines additional backpressure can decrease engine power by ~1% per inch Hg.²⁷ A specific exhaust heat exchanger design would need to take this effect into account to present a net system efficiency increase. Poor heat exchanger design has the potential to negate any net power recovery through decrease prime power conversion efficiency.

3.3 WHR Model Comparison

Goncalves et al.¹⁶ built a computational model of a cross-flow WHR system with the TEG hot sides mounted to a solid copper heat spreading block. Despite the fact that modeling results showed large thermal gradients (87.5 K/m) along the axial length of the copper block, their analysis assumed constant hot and cold side temperatures, and TE properties were calculated based on the average of the hot and cold side temperatures. While calculating the appropriate coolant mass flow rate necessary to reject the estimated 39 kW, the authors neglected any consideration of thermal resistances in the heat path from the TEG cold side to the fluid in the coolant loop. By assuming the TEG cold sides were maintained at the average coolant temperature (325 K), they essentially assume $R_{cool} = 0$ K/W, which is most certainly not the case. Applying these conditions and assumptions to our model, agreement is within 7%.

As noted previously, we arrive at $R_{cool} = 0.625$ K/W using a generous convection coefficient of 1000 W/m²K. Further reduction in R_{cool} is non-trivial and will add to the complexity and cost of the coolant loop. As a result of this assumption in Goncalves et al.,¹⁶ the power generation and efficiency of the TEG array is vastly overstated—they estimate the power generation by the TEG array to be 1530 W at a TEG conversion efficiency of 3.9%. Running the cross-flow model developed in this work with boundary conditions identical to Goncalves et al.¹⁶ except for using $R_{cool} = 0.625$ K/W, we estimate $P_{gen} = 48.2$ W at 0.4% efficiency. This discrepancy is primarily due to the TEG cold side temperatures—their model assumes these to be 325 K, while our more realistic case estimates them to average 427 K. Not only does this affect P_{gen} through $T_H - T_C$ (Eq. 6), but the TE properties also change.

4. Conclusion

This study considers the temperature load-leveling capability of integrated heat pipes and spreaders in a vehicle engine exhaust WHR system using TEGs. While simple, this study highlights important points to consider when designing such a system:

1. TEG properties are extremely sensitive to temperature. Designing a WHR system for a single operating point will lead to very poor performance when applied to a real system, as temperature fluctuations drastically change the TE material ZT.
2. Development of higher temperature, higher ZT TE materials will make WHR more practical. In systems using commercially available TE materials, much exhaust enthalpy is wasted because the TE performance is so poor at elevated temperatures (~800–1100 K).
3. Integrating heat pipes and spreaders in the cross-flow heat exchanger system provides very good temperature load leveling, which holds promise for future WHR applications. The downside is that extracting and transporting heat from the exhaust stream to the TEG hot sides requires very low thermal resistance paths. Inserting multiple heavily finned heat sinks into the exhaust stream will obstruct the flow and could lead to elevated backpressures and decreased engine performance.
4. Many studies in the literature make poor assumptions regarding system operating conditions and TE material properties, which leads to overestimated results. Rectifying this issue will require investments in both improved system-level modeling, accounting for the full heat flow path under realistic usage conditions, and experimental work to produce validated performance profiles of integrated WHR system components.

5. References

1. Fu G, Zuo L, Longtin JP. Review of waste energy resource in vehicle engine exhaust. Proceedings of ASME Summer Heat Transfer Conference; 2012, 58455.
2. Saqr KM, Musa MN. Critical review of thermoelectric in modern power generation applications. Thermal Science. 2009;13:165–174.
3. Crane DT, LaGrandeur JW. Progress report on BSST-led US Department of Energy automotive waste heat recovery program. Journal of Electronic Materials. 2009;39:2142–2148.
4. Sprouse III C, Depcik C. Review of organic Rankine cycles for internal combustion engine exhaust waste heat recovery. Applied Thermal Engineering. 2013;51:711–722.
5. He M, Zhang X, Zeng K, Gao K. A combined thermodynamic cycle used for waste heat recovery of internal combustion engine. Energy. 2011;36:6821–6829.
6. Hendricks TJ, Lustbader JA. Advanced thermoelectric power system investigations for light-duty and heavy duty applications: Part II. Proceedings of the 21st International Conference on Thermoelectronics; 2002, pp. 387–394.
7. Karri MA, Thacher EF, Helenbrook BT. Exhaust energy conversion by thermoelectric generator: Two case studies. Energy Conversion and Management. 2011;52:1596–1611.
8. Matsubara K. Development of a high efficient thermoelectric stack for a waste exhaust heat recovery of vehicles. Proceedings of the IEEE 21st International Conference on Thermoelectronics; 2002, pp. 418–423.
9. La Grandeur J, Crane D, Hung S, Mazar B, Eder A. Automotive waste heat conversion to electric power using skutterudite, TAGS, PbTe and BiTe. Proceedings of IEEE International Conference on Thermoelectrics; 2006, pp. 343–348.
10. Hsu C-T, Huang G-Y, Chu H-S, Yu B, Yao D-J. Experiments and simulations on low-temperature waste heat harvesting system by thermoelectric power generators. Applied Energy. 2011;88:1291–1297.
11. Hsiao YY, Chang WC, Chen SL. A mathematic model of thermoelectric module with applications on waste heat recovery from automobile engine. Energy. 2010;35:1447–1454.

12. Ceraianu MO, Gontean A. Parasitic elements modelling in thermoelectric modules. *IET Circuits Devices Systems*. 2013;7:177–184.
13. Matsubara K. Development of a high efficient thermoelectric stack for a waste exhaust heat recovery of vehicles. *Proceedings of the IEEE 21st International Conference on Thermoelectronics*; 2002, pp. 418–423.
14. Fu G, Zhang B, Zuo L, Longtin JP, Sampath S. Heat transfer modeling and geometry optimization of TEG for automobile applications. *Proceedings of the ASME Summer Heat Transfer Conference*; 2012, 58454.
15. Vijayagopal R, Shidore N, Reynolds M, Folkerts C, Rousseau A. Fuel displacement potential of a thermoelectric generator in a conventional vehicle. *Proceedings of IEEE Electric Vehicle Symposium and Exhibition*; 2013, pp. 1–6.
16. Goncalves LM, Martins J, Antunes J, Rocha R, Brito FP. Heat-pipe assisted thermoelectric generators for exhaust gas applications. *Proceedings of ASME International Mechanical Engineering Congress & Exposition*; 2010, 40926.
17. Parlak A. The effect of heat transfer on performance of the Diesel cycle and exergy of the exhaust gas stream in a LHR Diesel engine at the optimum injection timing. *Energy Conversion and Management*. 2005;46:167–179.
18. Chao S-I, Vining RA. Thermoelectric systems incorporating rectangular heat pipes. United States patent US 44480208. 1984.
19. Brito FP, Martins J, Goncalves LM, Sousa R. Temperature controlled exhaust heat thermoelectric generation. *SAE International Journal of Passenger Cars – Electronics and Electrical Systems*. 2012;5:561–571.
20. Incropera FP, DeWitt DP. *Fundamentals of heat and mass transfer*. New York (NY): Wiley; 2002.
21. Heat Pipes. Advanced Cooling Technologies, Inc; 2015 [accessed 2/1/2015]. <http://www.1-act.com/advanced-technologies/heat-pipes/>.
22. Heat Spreaders. Novel Concepts, Inc; 2014 [accessed 2/2/2015]. <http://www.novelconceptsinc.com/heat-spreaders.htm>.
23. Bradie B. *A Friendly Introduction to Numerical Analysis*. New Jersey: Prentice Hall; 2006.
24. Ethylene Glycol Heat-Transfer Fluid. The Engineering Toolbox; n.d. [accessed 9/1/2014]. http://www.engineeringtoolbox.com/ethylene-glycol-d_146.html.

25. Olier C, Oliva A, Castro J, Perez-Segarra CD. Parametric studies on automotive radiators. *Applied Thermal Engineering*. 2007;27:2033–2043.
26. Min G. Conversion efficiency of thermoelectric combustion systems. *IEEE Transactions on Energy Conversion*. 2007;22:528–534.
27. Adams TG. Effect of exhaust system design on engine performance. 1980. SAE Technical Paper No. 800319.

1 DEFENSE TECHNICAL
(PDF) INFORMATION CTR
DTIC OCA

2 DIRECTOR
(PDF) US ARMY RESEARCH LAB
RDRL CIO LL
IMAL HRA MAIL & RECORDS
MGMT

1 GOVT PRINTG OFC
(PDF) A MALHOTRA

2 DIRECTOR
(PDF) US ARMY RESEARCH LAB
RDRL SED EI
CP MIGLIACCIO
NR JANKOWSKI